Journal of Thermal Analysis and Calorimetry, Vol. 96 (2009) 2, 403–406

GLASS FORMING ABILITY AND THERMAL STABILITY OF OXYFLUORIDE GLASSES

A. R. Marquesi, J. R. J. Delben[*] *and A. A. S. T Delben*

Department of Physics, Federal University of Mato Grosso do Sul, 79070-900, Campo Grande, MS, Brazil

New oxyfluoride glasses based on the system ZrO_2–Pr_2O_3–ZrF_4–BaF_2 were obtained, and the glass forming ability of this system was evaluated. The effects of glass composition on both thermal stability and the crystalline phases formed upon heat treatment were determined by the DSC and XRD methods, respectively. The composition with higher thermal stability and better glass forming ability contained 2 mol% of oxides.

Keywords: *crystalline phase, oxyfluoride glass, thermal stability*

Introduction

Oxyfluoride glass fibers doped with rare earth have been developed for optical amplifiers and up-conversion devices. A low phonon energy host is required to improve luminescent efficiency of the rare earth ions. A vitreous fluoride matrix is generally preferred over an oxide one, due to both the lower phonon energy and the higher rare earth solubility of the fluoride glass [1, 2]. However, the drawback of the fluoride glass is its poor chemical and thermal stability. Transparent glass-ceramics possess more attractive optical properties than glass fibers and a simpler production process than single-crystal optical fibers [3]. The aim of fluoride-oxide association is to obtain materials with better optical properties than oxide and improved thermal properties compared to fluoride glasses. The nanocrystalline phase can be produced in glassy samples under heat treatment [4], and the crystal size and segregation conditions influence luminescent emission [3, 5]. Many researchers have developed oxyfluoride glass-ceramics doped with trivalent optical active elements [6–9]. The composition of glass-ceramics, their crystalline dimensions and phases and the dopant amount influence the properties of the materials and determine their applications [10–16]. Thus, to prepare glass-ceramics with the desired microstructure and properties, knowledge of the thermal behavior of the materials is of great significance [17–20]. In this work, new glasses of the system ZrO_2–Pr_2O_3–ZrF_4–BaF_2 were prepared. The ternary vitreous domain of ZrF_4–BaF_2–PrF_3 was previously determined [21], and vitreous samples could be obtained in the range (50–78)ZrF_4–(20–40)BaF_2–(3–20)PrF_3 in mol%. In this work, oxides were added to this system, replacing the PrF_3 and part of ZrF_4. The thermal stability parameters were calculated from DSC curves. The crystallization evolution as a function oxide content was analyzed by XRD.

Experimental

Oxyfluoride glasses of the system $x(0.96ZrO_2+0.04Pr_2O_3)$–$[100–(x+y)]ZrF_4$–$yBaF_2$, (were x=0–4 and y=27.5–43) in mol% were prepared. The fluoride raw materials were ZrF_4 and BaF_2 – 99.9%-Fluortran Grade-BDH from Merck; the oxides ZrO_2 and Pr_2O_3 were also 99.9% from Merck. The batches were melted in a platinum crucible at 850°C for 30 min in a dry box filled with nitrogen. To determine the vitreous domain, the samples were prepared by splat cooling. For the compositions with higher glass forming ability, samples with dimensions of 10.0×15.0×3.0 mm were prepared. They were poured into a brass mold and annealed for 30 min at T_g.

The glass transition onset temperature (T_g), the crystallization onset temperature (T_x), and the crystallization peak temperature (T_p) were obtained from DSC curves. The measurements were run in Shimadzu-50TA equipment. The milled samples (5 mg), with particles ranging between 420 and 590 μm, were placed in a platinum crucible in a nitrogen flux of 100 mL min^{-1} and heated at the rate of 10°C min^{-1}. For particles smaller than 250 μm, superficial crystallization takes place, and peak positions shift drastically in each experiment. Meanwhile, for larger particles, bulk crystallization dominates, and peak positions are not detectably affected [22–25]. The thermal stability parameter $\Delta T=T_x-T_g$ was also calculated.

---

[*] Author for correspondence: delbenbr@yahoo.com.br

1388–6150/$20.00

Akadémiai Kiadó, Budapest, Hungary
Springer, Dordrecht, The Netherlands

Samples containing 35 mol% of BaF_2 and either 0, 2, 2.5, 3 or 4 mol% of oxides were heated for 60 min at T_p to investigate the crystalline phases present. Diffraction X-ray was performed with a Rigaku-Rotaflex RINT2000 – CuK_α radiation, and the patterns were analyzed using the ICSD (Inorganic Crystal Structure Database).

Results and discussion

The samples of the system $x(0.96ZrO_2+0.04Pr_2O_3)$–$[100–(x+y)]ZrF_4$–$yBaF_2$, with x=0-4, in mol% were prepared by splat cooling, and they were classified according to the presence and intensity of crystallization, Fig. 1. Samples vitrified in the range of $(56–73)ZrF_4$–$(28–43)BaF_2$–$(0–4)(ZrO_2$-$Pr_2O_3)$ in mol%.

Bulk samples of the system $x(0.96ZrO_2–0.04Pr_2O_3)$–$(65–x)ZrF_2$–$35BaF_2$, with x=0–4 in mol% were also prepared. The samples with 35 mol% of BaF_2 and 2 mol% of oxides vitrified more easily. The vitreous samples, prepared by splat cooling, were then analyzed by DSC, and these crystallization curves are presented in Fig. 2.

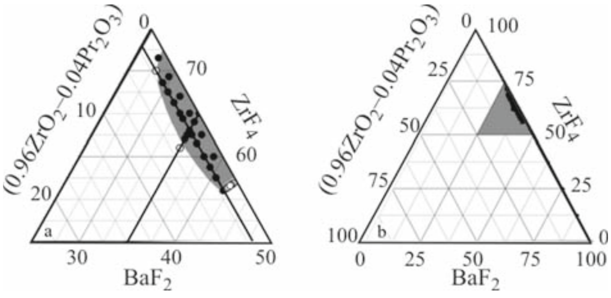

Fig. 1 Vitreous diagram for samples of the system $x(0.958\ ZrO_2+0.042Pr_2O_3)$–$[100–(x+y)]ZrF_4$–$yBaF_2$, in mol%, with x=0–4 mol%. ● – glass; ○ – glass-ceramics, a is the dark area of b

For samples containing 1 mol% of oxides, the crystallization occurred at two distinct temperatures, 360 and 374°C. For samples containing 2 and 3 mol% of oxides, there was a superposition of the two crystallization peaks, while the samples with 4 mol% of oxides showed only one peak at 376°C.

The inclusion of oxides and their covalent bonds caused an increase in T_g, as seen in Fig. 3. This was associated with increasing viscosity of the melted material, a fact observed during sample preparation. The temperatures T_x and T_p increased rapidly with increasing oxide content up to the level of 2.0–2.5 mol% of oxides. Beyond this content, T_p became practically constant, while T_x presented a local minimum at 3 mol% of oxides, followed by an overall tendency to increase, though at lower rate.

In the range of 0–2.5 mol% of oxides content, the thermal stability parameter increased rapidly with oxide addition, though there was a local minimum for 3 mol% of oxide, as seen in Fig. 4. The covalent bonds associated with the oxide stabilize the glass matrix. This fact agrees with the confusion principle used for fluoride glasses: the greater the number of chemical elements, the greater the glass stability against devitrification, since varied elements induce competition between the different crystalline phases that can be formed [26, 27]. For samples up to 2.5 mol% of oxides, two crystallization peaks were observed, and thermal stability tended to increase.

For 4 mol% of oxides, there was only one narrow and intense crystallization peak, and thermal stability no longer increased. This fact could be associated with the oxide solubility limit to form glasses in the fluoride matrix, and it could also be related to the increasing rates of nucleation and crystal growth in the melting. Samples with 4 mol% of oxides were very difficult to prepare in a vitreous state, and no sample could be obtained with higher oxides content.

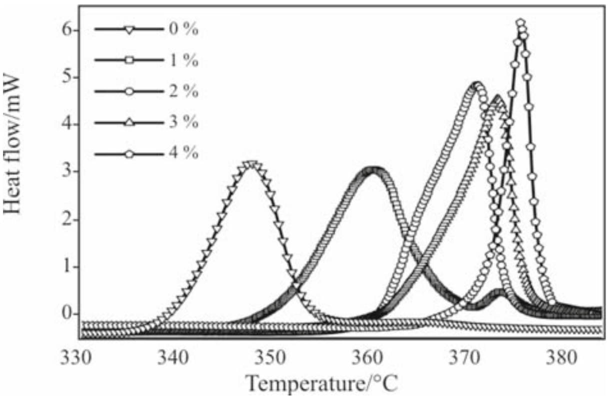

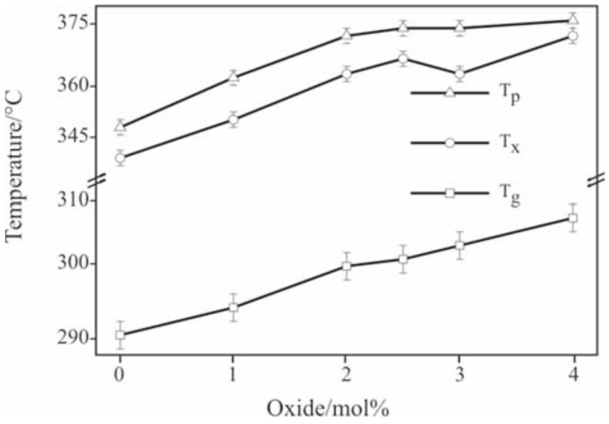

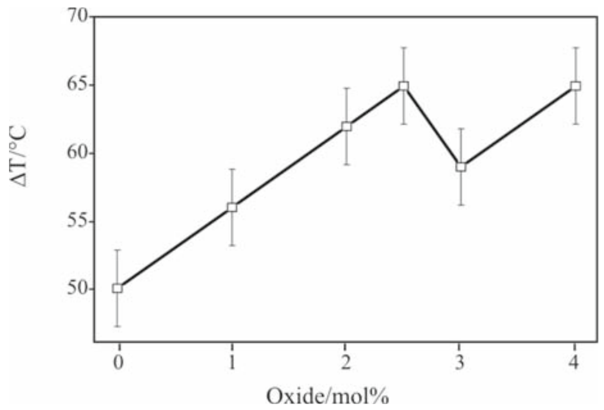

Fig. 4 Thermal stability parameter ΔT for samples containing 35 mol% of BaF_2 and different amounts of oxides and ZrF_4. The interpolating line is a guideline

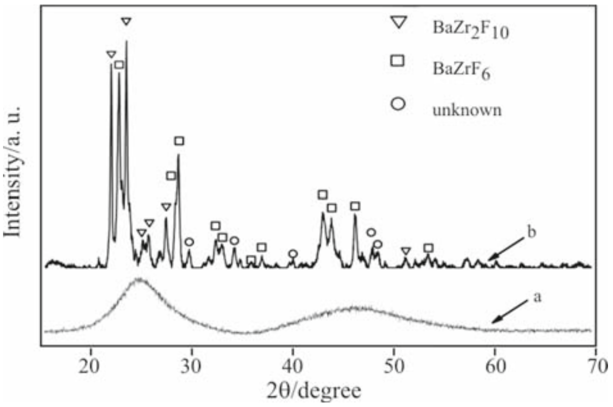

Fig. 5 XRD of glass with composition: a – $2(0.92ZrO_2+0.08Pr_2O_3)$–$63ZrF_2$–$35BaF_2$ in mol% and b – of the same sample after heating for 30 min at T_x

Figure 5 presents a typical XRD curve for the sample containing 2 mol% of oxides, showing no crystallization of the samples before heat treatment. The other compositions, excepting the glasses containing 4 mol% of oxides, presented similar XRD patterns. The crystalline phases α-$BaZr_2F_{10}$ (file 000-39-1047), β-$BaZr_2F_{10}$ (files 000-38-0776 and 000-40-0987) and β-$BaZrF_6$ (files 000-40-0985 and 000-40-0986) were identified (files of the ICSD) in samples with 1–3 mol% of oxides and 35 mol% of BaF_2 and also for the reference sample with no oxide and 34 mol% of BaF_2. For the sample with 4 mol% of oxides, only the β-$BaZrF_6$ phase was present, Fig. 6, as expected from the DSC curve which showed only one crystallization peak. Thus, for the samples with 1–3 mol% of oxides, the phase $BaZr_2F_{10}$ crystallizes at a lower temperature.

Our XRD results agreed with the results of other authors. Namely, we found that in fluorozirconate glasses, zirconium can coordinate as ZrF_5^- and ZrF_6^{2-}; in association with BaF_2, it can crystallize as $BaZr_2F_{10}$ and $BaZrF_6$ [28–31].

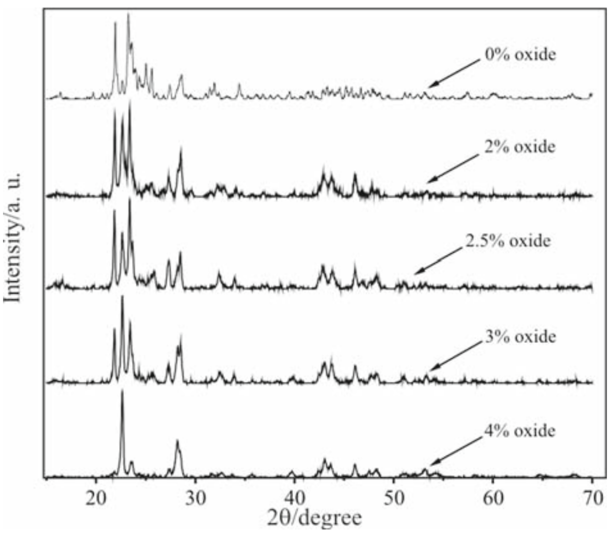

Fig. 6 XRD patterns of samples with different oxides content heated for 30 min at T_x

Conclusions

Glass samples with new compositions of the system ZrO_2–Pr_2O_3–ZrF_2–BaF_2 were prepared. Glasses formed in the range (56–73)ZrF_4–(28-43)BaF_2–(0–4)(ZrO_2–Pr_2O_3) in mol%, but glass forming ability decreased beyond 2 mol% of oxides. The best composition, according to both the criteria of glass forming ability and higher thermal stability, was $2(0.92ZrO_2+0.04Pr_2O_3)$–$63ZrF_2$–$35BaF_2$, in mol%. The thermal stability increased with oxides content up to 2.5 mol% of oxides, though decreasing slightly for 3 mol% of oxides. Upon heating, the samples with up to 3 mol% of oxides crystallized in the phases α-$BaZr_2F_{10}$, β-$BaZr_2F_{10}$ at lower temperature, and they crystallized as β-$BaZrF_6$ at higher temperature. Samples with 4 mol% of oxides were difficult to vitrify, and upon heating only the β-$BaZrF_6$ phase crystallized. No vitreous sample could be obtained for oxide content above 4 mol%.

Acknowledgements

The authors are thankful for financial support from FINEP/CTINFRA-04, CNPq and UFMS.

References

1 D. Chen, Y. Wang, E. Ma, Y. Yu and F. Lin, Opt. Mater., 29 (2007) 1693.
2 M. Mortier and F. Auzel, J. Non-Cryst. Solids, 256 and 257 (1999) 361.

3 G. Dantelle, M. Mortier and D. Vivien, Phys. Chem. Chem. Phys., 9 (2007) 5591.
4 M. Reben, I. Wactawska, C. Paluszkiewicz and M. Sroda, J. Therm. Anal. Cal., 88 (2007) 285.
5 F. Bao, Y. Wang and Z. Hu, Mater. Res. Bull., 40 (2005) 1645.
6 L. N. Ignatieva, N. V. Surovtsev, V. G. Plotnichenko, V. V. Koltachev, E. B. Merkulov, S. A. Polyshchuk and V. M. Bouznik, J. Non-Cryst. Solids, 353 (2007) 1238.
7 J. Méndez-Ramos, V. K. Tikhomirov, V. D. Rodriguez and D. Furniss, J. Alloys Compd., 440 (2007) 328.
8 T. Murakami and S. Tanabe, J. Ceram. Soc. Jpn., 115 (2007) 605.
9 F. Liu, D. Chen, Y. Wang, E. Ma and Y. Yu, J. Alloys Compd., 443 (2007) 143.
10 M. J. Dejneka, J. Non-Cryst. Solids, 239 (1998) 149.
11 Z. Hu, Y. Wang, F. Bao and W. Luo, J. Non-Cryst. Solids, 351 (2005) 722.
12 W. Choi and A. Manthiran, Solid State Ionics, 178 (2007) 1541.
13 Z. C. K. Bouchaour, M. Poulain, M. Belnadji, I. Hager and R. El Mallawany, J. Non-Cryst. Solids, 351 (2005) 818.
14 M. Sroda, I. Waclawska, L. Stock and M. Reben, J. Therm. Anal. Cal., 77 (2004) 193.
15 A. B. Seddon, V. K. Tikhomirov, H. Rowe and D. Furniss, J. Mater. Sci. Mater. Electron, 18 (2007) 145.
16 S. Yonezawa, S. Nishibu, M. Leblanc and M. Takashima, J. Fluor. Chem., 128 (2007) 438.
17 M. Sroda, J. Therm. Anal. Cal., 88 (2007) 245.
18 F. Auzel, D. Pecile and D. Morin, J. Electrochem. Soc., 122 (1975) 101.
19 F. Goutaland, P. Jander, W. S. Brocklesby and G. J. Dai, Opt. Mater., 22 (2003) 383.
20 J. R. J. Delben, A. A. S. T. Delben, K. Miazato, S. L. Oliveira and Y. Messaddeq, J. Therm. Anal. Cal., 75 (2004) 637.
21 J. R. J. Delben, D. R. Chaves, P. D. Candelório and A. A. S. T. Delben, J. Therm. Anal. Cal., 83 (2006) 411.
22 V. C. S. Reynozo, K. Yukimitu, T. Nagami, C. L. Carvalho, J. C. S. Moraes and E. B. Araújo, J. Phys. Chem. Solid, 64 (2003) 27.
23 C. S. Ray and D. E. Day, J. Am. Ceram. Soc., 73 (1990) 439.
24 J. Xiaojie, C. S. Ray and D. E. Day, J. Am. Ceram. Soc., 74 (1991) 909.
25 C. S. Ray, W. Hung and D. E. Day, J. Am. Ceram. Soc., 74 (1991) 60.
26 B. Cantor, I. T. H. Chang, P. Knight and A. J. B. Vicent, Mater. Sci. Eng., 375 (2004) 213.
27 X. Gu, L. Q. Xing and T. C. Hufnagel, J. Non-Cryst. Solids, 311 (2002) 77.
28 E. I. Voit, A. V. Voit and V. I. Sergienko, Glass Phys. Chem., 27 (2001) 195.
29 E. I. Voit, A. V. Voit, A. V. Gerasimenko and V. I. Sergienko, J. Struct. Chem., 41 (2000) 41.
30 N. P. Bansal, R. H. Doremus, A. J. Bruce and C. T. Moynihan, Mater. Res. Bull., 19 (1984) 577.
31 Y. Kawamoto and F. Sakaguchi, Bull. Chem. Soc. Jpn., 56 (1983) 2138.

Received: May 6, 2008
Accepted: September 10, 2008
Online First: January 12, 2009

DOI: 10.1007/s10973-008-9218-5